JOURNAL OF GEOPHYSICAL RESEARCH, VOL. 103, NO. C13, PAGES 30,985–31,002, DECEMBER 15, 1998

Mean circulation and transports in the South Atlantic Ocean: Combining model and drifter data

S. Stutzer and W. Krauss
Institut für Meereskunde Kiel, Kiel, Germany

Abstract. Numerical experiments with a medium-resolution primitive equation model of the South Atlantic mean circulation are described. The results from the standard model realization indicate that the model succeeds in representing the large-scale transport and circulation features. However, a comparison with a velocity field derived from surface drifter data reveals discrepancies of the modeled velocities from the observations in magnitude as well as direction of the flow field. In order to diminish the model deviations from the data, an attempt is made to couple the model to the observations through a simple data assimilation technique. The assimilated model succeeds in improving the subtropical gyre circulation. Only a minor effect on the basin-scale integrated quantities is observed. However, the density field may be deformed as a response to the assimilation of velocity data without simultaneously adapting a corresponding density structure. The influence of the disturbance of the density structure is most prominent at the edges of the observed data set, which does not cover the entire model domain, and is confined to the upper ocean and balanced above the thermocline. We calculated a meridional heat transport that is generally in accordance with estimates from other sources. The analysis of heat and salt fluxes suggests that the model features both the so-called "warm water path" and "cold water path" in closing the global thermohaline circulation. While heat is mainly imported in surface and thermocline waters with the Agulhas Current around South Africa, it is the Antarctic Intermediate Water that compensates for more than 50% of the salt loss by the outflowing North Atlantic Deep Water.

1. Introduction

The circulation of the South Atlantic Ocean is characterized by complex features that result from the various water exchange processes with the adjacent oceans. The South Atlantic connects the North Atlantic Ocean with the South Pacific and the South Indian Ocean, respectively. Thus it constitutes an area of key importance for the oceanic branch of the global cycles of heat and freshwater. The communication of the South Atlantic with the Pacific is restricted to the relatively narrow Drake Passage, where the Antarctic Circumpolar Current (ACC) penetrates the South Atlantic with a net transport of the order of 130 Sv (1 sverdrup = 10^6 m^3/s) [see *Whitworth and Peterson*, 1985; *Whitworth et al.*, 1982]. Unlike the situation at its western boundary, the South Atlantic has a wide open boundary to the Indian Ocean, where outflow from the Atlantic as well as inflow into the Atlantic occur. The relatively short southward extension of the African continent allows a direct communication of the western boundary current of the South Indian Ocean (Agulhas Current) with the South Atlantic. Within the South Atlantic itself the bottom topography and the interaction of the zonal ACC with the subtropical South Atlantic have an impact on the flow field and the water mass characteristics. As a consequence, the circulation is governed by a wide range of interacting processes from small-scale eddies to the long-term themohaline circulation. The eddies have a crucial importance for water mass transformation in the Brazil-Malvinas Current Confluence Zone (BMCZ) and for the interocean exchange of thermocline waters with the Indian Ocean in the Agulhas Retroflection area. The small-scale eddies may contribute to the large-scale thermohaline circulation that is often described in an idealized picture. It states that the abyssal layers of the South Atlantic represent a transition region for the North Atlantic Deep Water (NADW) that is formed in the northern North Atlantic and is spreading into the world ocean via the South Atlantic, where it joins the ACC. Near the surface there must be a recirculating pathway for thermocline and intermediate waters from the Indian and Pacific Oceans into the South Atlantic. These water masses are eventually transferred into the North Atlantic to compensate for the outflowing NADW, thus closing the global thermohaline circulation cell. This schematic flow is not directly observable on its entire path because of the long timescales involved and the dilution of the water mass characteristics through mixing and water mass transformations. However, modeling the ocean circulation may lead to an identification of the prevalent path of the recirculating flow into the North Atlantic and give some clues on the control mechanisms and the stability of this flow.

There are generally two possible approaches to modeling the circulation of the South Atlantic Ocean. One is to consider it as a subdomain of a global or hemispheric model. Examples are the eddy-resolving models of *Semtner and Chervin* [1992] and the United Kingdom Fine Resolution Antarctic Model (FRAM) [see *The FRAM Group*, 1991] or the global, not eddy-permitting model of *England and Garçon* [1994]. A different strategy is to compute a basin-scale model of the South Atlantic Ocean. Then the processes at the large open boundaries to the adjacent oceans have to be simulated by the model accord-

Paper number 98JC02065.
0148-0227/98/98JC-02065$09.00

Table 1. Model Grid and Mixing Coefficients

Value	Parameter	Definition
dx	1.2°	zonal resolution
dy	1.0°	meridional resolution
Nz	30	number of levels
dt	1 hour	time step
	Subgridscale Mixing Coefficients, cm²/s	
A_{MH}	1.0×10^8	horizontal viscosity
A_{HH}	5.0×10^6	horizontal diffusion
A_{iso}	1.0×10^7	isopycnal diffusion
A_{MV}	10.0	vertical viscosity
A_{HV}	0.3	vertical diffusion

ingly. While, in global models, the processes in the transition region from one ocean to another are entirely determined by the model itself, they have to be parameterized by open boundary conditions in limited area models. On the other hand, the spatial limitation allows one to carry out numerical experiments at much lower computational costs than with a global model.

The model results presented in this paper fit into the latter group of models. As our main objective is the determination of the mean circulation of the South Atlantic and the meridional transports, we use a noneddy-resolving, primitive equation model. The model complements the previously obtained results from different South Atlantic models, notably those of *Marchesiello et al.* [1998] and *Marchesiello* [1995], who make use of the semispectral primitive equation model (SPEM) [see *Haidvogel et al.*, 1991] (and the study of *Matano* [1993]). Matano presents results obtained by using the same model type as in this paper, but with an emphasis on the physics of the Brazil-Malvinas Confluence Zone.

We show first that the limited area, noneddy-resolving model with large lateral open boundaries and simple open boundary conditions is capable of simulating the large-scale circulation of the South Atlantic Ocean and related quantities reasonably well in comparison with results from other models. This is shown notably through a presentation of heat and volume transports. We analyze, in a more detailed discussion, the importance of water transfers from the Pacific and the Indian Oceans into the South Atlantic.

In addition to a model intercomparison, model results have to be validated with observed quantities. Yet direct observations of the hydrography and flow field below the sea surface in the South Atlantic are still relatively scarce (apart from nearshore areas and the boundary current regimes). The database consists mainly of cross-Atlantic hydrographic sections and Lagrangian observations from surface drifters and subsurface floats. Thus, in the past, a validation of model results was done mainly by comparison with either climatological data sets [*Levitus*, 1982] or regionally available observations. In this paper we use a velocity field derived from a surface drifter data set for this purpose. Because this comparison revealed some differences between the modeled and observed flow fields, an additional step was undertaken by assimilating the velocity observations into the model, thus reducing the model-data decrepancies. This is the second aim of this work: to study the influence of the assimilation of an observed velocity field in a single model layer on the three-dimensional circulation and hydrography of the model.

The paper is organized as follows: the model and the assimilation method (both are commonly used in numerical modeling) are briefly discussed in section 2. Some aspects of the standard or reference experiment are presented in section 3. It is shown that the model reproduces the essential features of the South Atlantic hydrography and circulation. However, as discussed in section 4, differences between a mean velocity field derived from drifter data and the model results appear in the representation of the mean flow in 100 m depth. The assimilation of the observed data leads to a reduction of this discrepancy and affects the meridional transports of volume and heat as discussed in section 5. Finally, in section 6, results from the reference and assimilation experiments are reviewed with respect to the role of the South Atlantic in the global circulation. The pathways of the surface and intermediate waters into the North Atlantic are discussed in this context.

2. Model

The numerical model used in this study is based on the z coordinate, primitive equations. It was developed at the Geophysical Fluid Dynamics Laboratory (GFDL) and is described by *Bryan* [1969]. The code was further developed notably by *Cox* [1984], who adapted the model for use on vectorizing computers, and by *Pacanowski et al.* [1991, 1995], who introduced the model in its modular formulation. The reader is referred to these authors for a complete description of model physics and numerics.

The model domain extends from 74°W to 46°E and from 78°S to 12°N. The horizontal resolution is 1.2° and 1° in zonal and meridional directions, respectively. The vertical axis is resolved in 30 levels. Below 1000 m depth the level thickness is 250 m; in the upper ocean, layer thickness rises from 35 m in the top layer to 198 m above 1000 m depth. Bottom topography was taken from the 1° bathymetry data set of the Scripps Institution of Oceanography. Constant coefficients of diffusivity and viscosity have been chosen as listed in Table 1. Isopycnic mixing is parameterized as described by *Redi* [1982].

Processes at an open boundary are parameterized as follows: in the case of an inflow, the water mass properties at the boundary are unbiased by the interior model solution and climatological data for salinity and temperature are prescribed. For outward directed flow, model temperature and salinity are relaxed to climatological values inside a boundary layer. This extends over the five grid rows adjacent and parallel to the respective edge. At the boundary itself the tracer values are again prescribed from climatological data. An additional increase of the coefficients for diffusion and viscosity inside the boundary zone dampens outward directed disturbances and suppresses reflections at the boundary. The coefficients rise with an e-folding scale by a factor of 10 at the boundary compared with their interior values. The baroclinic flow at the boundaries is consistent with the tracer distribution, i.e., in geostrophic balance.

This rather simple boundary condition differs in many respects from the more sophisticated radiation boundary conditions [cf. *Stevens*, 1990, 1991]. In particular, it does not allow perturbations of the flow field explicitly to leave the model domain. Instead, they are dampened inside the sponge layer, close to a boundary. Reflections at the boundary may occur, nevertheless, but the penetration of a reflected wave into the model interior is unlikely because of the trapping effect of the boundary layer. However, the radiation condition has the clear advantage that the (simplified) model dynamics alone deter-

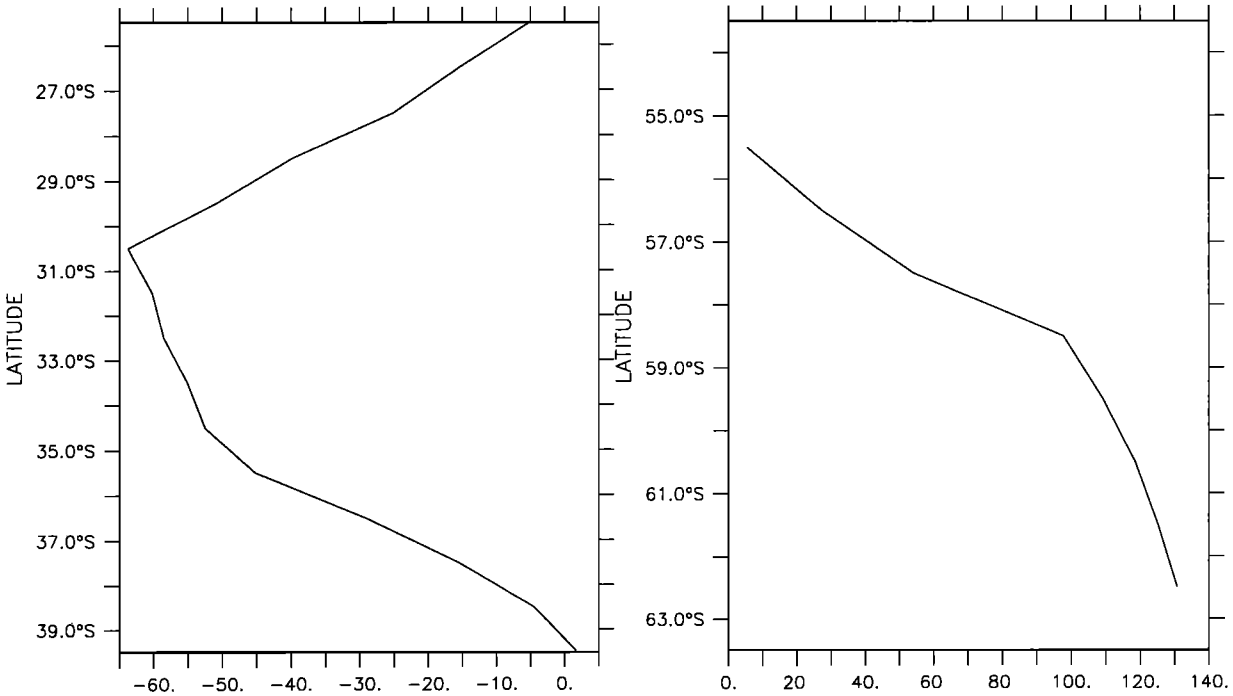

Figure 1. Meridional distribution of barotropic stream function (in sverdrups) at (left) eastern (Agulhas Current system) and (right) western (Drake Passage) open boundaries.

mine the boundary condition (in the outflow case), while in our model an additional (a priori unphysical) term forces the model solution to remain close to the prescribed climatological boundary values.

Both parameterizations are possible approaches to simulate open boundary processes in such a way that the model evolves largely unaffected away from the boundaries. This has been demonstrated by *Stutzer* [1997] in a comparison between our model with the simple boundary condition and in another model with *Stevens'* [1990, 1991] open boundary condition applied. The latter model is the 1° Community Modeling Effort (CME) model of the North Atlantic Ocean [*Döscher and Redler*, 1997] that overlaps the South Atlantic model between 15°S (southern boundary of the North Atlantic model) and 12°N (northern boundary of the South Atlantic model). Both simulations represent the hydrography and the interior flow field with similar results, indicating that the simulated circulation of the tropical Atlantic is only marginally sensitive to the specific open boundary condition applied.

Additional lateral boundary conditions are required for the barotropic stream function. In order to simulate the inflow and outflow of the ACC as well as of the Agulhas Current (AC) and Agulhas Return Current (ARC), the following cross-boundary transports have been prescribed: the ACC carries 130 Sv in Drake Passage and at 45°E, while the inflowing AC and the outflowing ARC balance each other by transporting 60 Sv each. The barotropic inflow is concentrated in the northern half of Drake Passage, as sketched together with the barotropic Agulhas Current System inflow and outflow profiles in Figure 1.

For the assimilation of velocity data into the model, we used the nudging technique that has been introduced into oceanography during the last decade and widely used since then (see, for example, *Holland and Malanotte-Rizzoli* [1989]). In the nudging formulation an additional term including the model-data difference of the respective variable is attached to the prognostic equation as demonstrated here for the zonal velocity component u

$$u_t = -p_x + fv + L(u) + A + \frac{1}{\tau_{\text{vel}}}(u_{\text{obs}} - u_{\text{mod}}) \qquad (1)$$

where v, p, and f are the meridional velocity component, pressure, and Coriolis parameter, respectively. Indices x and t indicate derivatives in the respective coordinate. The operator $L(u)$ includes the advective terms; A represents the parameterization of subgrid-scale processes. The meaning of the new term on the right-hand side is that the model is nudged toward the observed value by adding the difference between an observed velocity u_{obs} and the simulated velocity u_{mod}.

Directly observed velocity data have scarcely been used for assimilation into numerical models. Recent experiments of *Woodgate* [1997], who used simulated data for assimilation into the free-surface Bryan-Cox [*Bryan*, 1969; *Cox*, 1984] model, yielded rather discouraging results, since the assimilation in the baroclinic velocity components excites inertia-gravity oscillations with a high wave frequency that can be resolved by the baroclinic time step. Thus the model becomes numerically unstable if only velocities are assimilated in the baroclinic mode. However, the experiments that are discussed in this paper remained numerically stable for two reasons. First, we used the rigid lid approximation which eliminates the external high-frequency gravity mode. Second, as explained in detail below, the assimilation of velocity data was carried out continuously. The only time-varying part of the assimilation is a result of the model-data difference that varies (usually decreases) during the integration. Except for the onset of the assimilation when a planetary wave is generated as a barotropic response to the disturbance of the baroclinic velocity field, there are no wavelike disturbances created in the barotropic mode.

In our experiments the strength of the assimilation depends

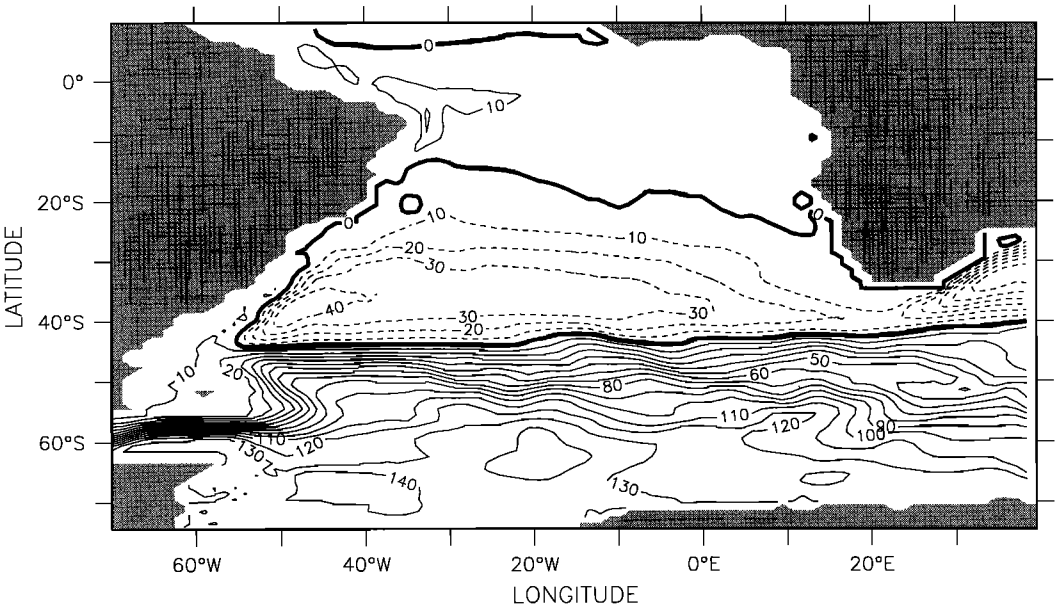

Figure 2. Mean barotropic stream function from the reference experiment. Numbers are in sverdrups.

on the model-data difference and on the timescale τ_{vel}, which itself is usually a function of time. We drop this time dependence and apply (1) in one single model level, since we are using just one data set in one depth. Finally, the parameter τ_{vel} is set to $\tau_{vel} = 6$ hours. As this timescale is rather short, it is expected that the nudging term might become of the same order of magnitude as the physical terms in (1). Sensitivity experiments [*Stutzer*, 1997] have shown that this term does indeed dominate the nonlinear and frictional terms of the momentum balance but is significantly smaller than the leading geostrophic terms, since the density field responds only slowly to the changed advection of salinity and temperature. The strong relaxation ensures that the directly affected model level adapts closely to the imposed velocity field without causing unrealistically large disturbances of the tracer fields. The consequences of this assimilation are discussed in section 5.

Results presented in this paper are obtained from two model realizations. Both were set up on the final state of a 25 year spin-up experiment that was started from an ocean initially at rest and with a tracer initialization adapted from the climatologies of *Levitus* [1982] and *Olbers et al.* [1992]. North of 30°S, the former data set was used; south of 35°S, we used exclusively the latter climatology which covers the Southern Ocean only. In the narrow zone in between, both data sets have been merged linearly. The differences between the climatologies (e.g., the Southern Ocean climatology generally resolves fronts better than the rather smooth Levitus data set) made it necessary to compute a relatively long spin-up experiment that allowed a baroclinic adjustment and adaptation of the model fields to the initial tracer distribution.

The first experiment, called the reference run, is merely a continuation of the spin-up and was integrated over an additional 10 years. Mean fields were computed using the last 5 years of that period. The second simulation, denoted the relaxation experiment, was run over 10 years, again using the last 5 years of the integration to compute annual averages. During the whole period of the relaxation experiment the observed data were assimilated as described above. The integration time is sufficiently long for the tracer and velocity fields in the upper ocean to adjust to the momentum forcing in one model layer. The first experiment was run for the same time span to obtain a consistent reference data set.

Both experiments (except for the data assimilation procedure) were identical. Thus the same forcing fields were used in the simulations: the surface wind forcing consisted of the monthly mean wind stress climatology from *Hellermann and Rosenstein* [1983]. Relaxations toward sea surface salinities [from *Levitus*, 1982] and apparent air temperature [from *Oort*, 1983] were used as the thermohaline boundary conditions at the sea surface.

3. Numerical Experiments: Reference Run

In this section the modeled mean flow field and hydrography from the reference run are presented. The mean barotropic stream function is depicted in Figure 2. While the ACC is mainly driven by its prescribed inflow of 130 Sv in the Drake Passage and its outflow between Africa and Antarctica, there is a well-established, wind-driven subtropical gyre to the north of the ACC. At its western edge the Brazil Current appears to be rather strong as a result of the southward flowing surface, intermediate, and deep water masses. The latitude of separation of the Brazil Current is about 45°S and thus shifted by approximately 7° too far to the south when compared with observations. The same feature is exhibited in the results of *England and Garçon* [1994] using the same model type with a likewise coarse horizontal resolution. This model behavior is a well-known effect of level models when using a coarse grid and can be avoided by a higher horizontal resolution as has been demonstrated, for example, by *Matano* [1993].

The eastern boundary current of the subtropical South Atlantic, the Benguela Current, is reproduced as a broad and weak one. It is partially fed by Indian Ocean thermocline water leaking from the AC. The contribution of Indian Ocean water into the South Atlantic through the Agulhas Current system amounts to approximately 15 Sv. This transfer rate is of the

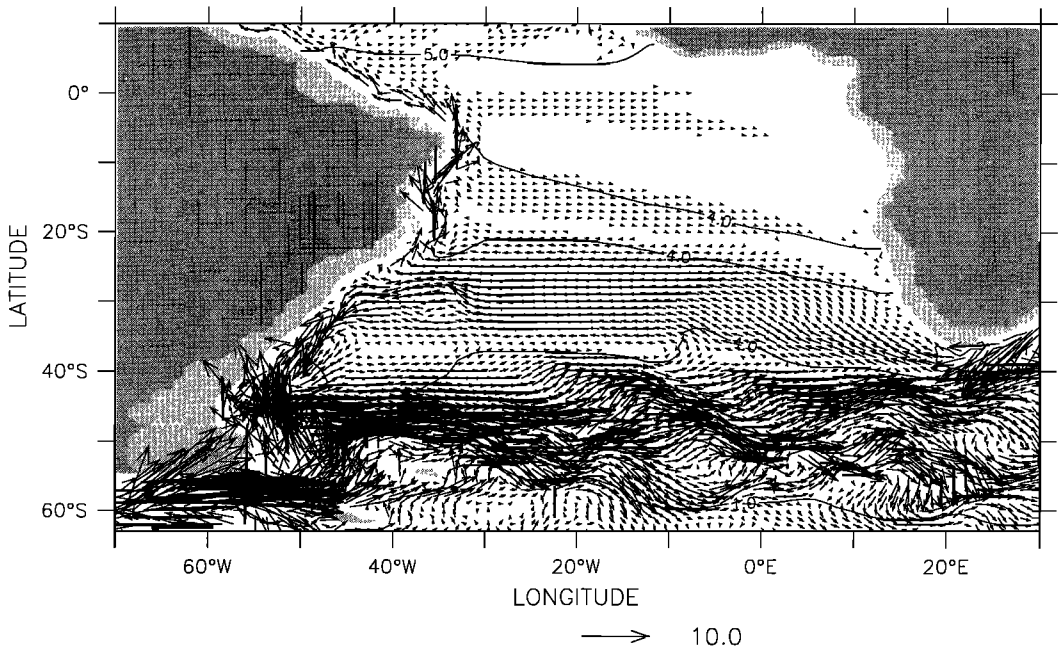

Figure 3. Velocity field and temperature distribution at 900 m depth from the reference experiment.

same order of magnitude as has been observed and reported, for instance, by *Clement and Gordon* [1995] and *Gordon et al.* [1992]. The value is in between other model estimates; it is much smaller compared with the FRAM results [*Thompson et al.*, 1997] but considerably higher than the 5–8 Sv inflow used by *Marchesiello* [1995] and *Matano and Philander* [1993] as an initial boundary value at 20°E.

To give an impression of the flow field as it is simulated by the reference model, consider the mean flow of Antarctic Intermediate Water (AAIW) in 900 m depth, depicted in Figure 3. It is characterized by the gyrelike spreading of AAIW between 20° and 40°S. The extended westward flow in the central and northern parts of the gyre (between 20° and 35°S) bifurcates at the South American shelf, near 30°S, into a northward branch that eventually leaves the South Atlantic and a southward, recirculating part below the near-surface Brazil Current. This gyre circulation is maintained by inflowing AAIW through the Agulhas Current system, while only a small fraction of AAIW is mixed into the subtropical gyre across the ACC.

The model also reproduces the distribution of tracers in a satisfying manner. In Figure 4 a meridional salinity section from the model is presented. It extends over the same latitudinal range as two hydrographic sections that were sampled in spring 1989 and analyzed by *Tsuchiya et al.* [1994]. When comparing the model results to actual hydrographic sections, one has to keep in mind that the model represents a spatially

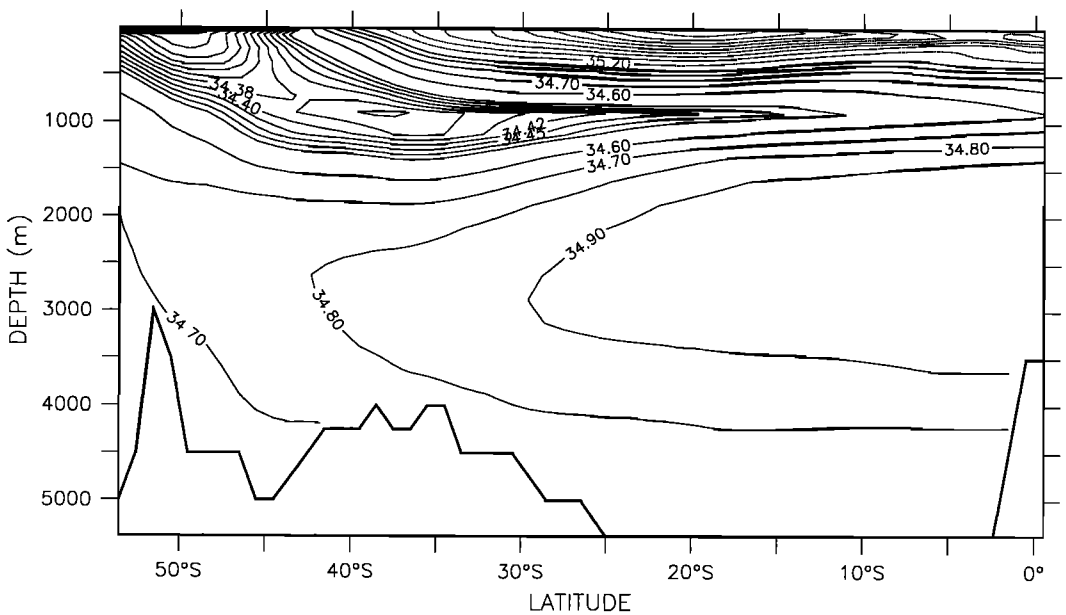

Figure 4. Salinity section along 25°W from 54°S to 1°N from the reference experiment.

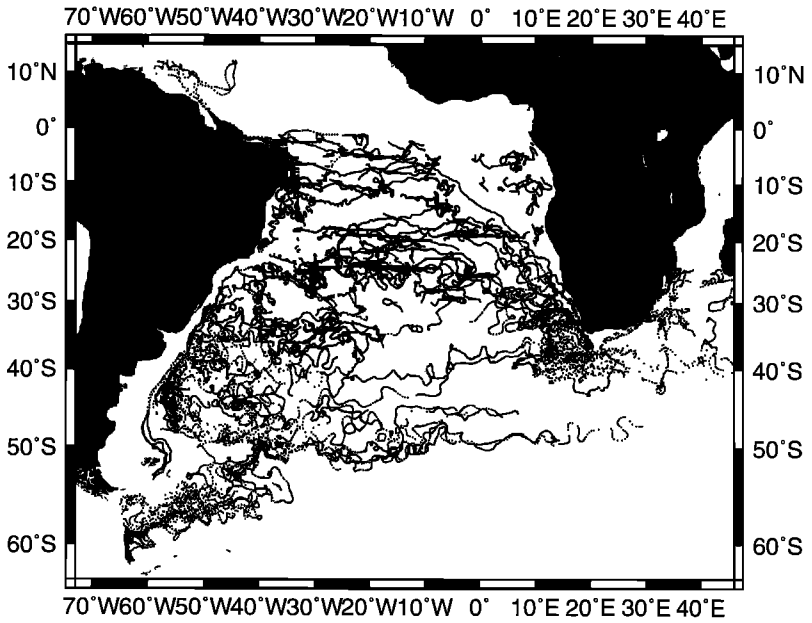

Figure 5. Trajectories of the World Ocean Circulation Experiment South Atlantic surface drift data set after rejecting data from undrogued buoys.

smooth, multiyear mean state on a coarse grid while the conductivity-temperature-depth (CTD) section resembles more a momentary snapshot. Thus the observed extreme values of salinity within the AAIW and NADW are not reproduced by the model, which naturally is also unable to simulate small-scale features that appear in the CTD section. Under these premises the model simulates the characteristics and meridional extension of the dominant water masses in close correspondence with the observation. That is, the vertical sequence of surface, intermediate, deep, and bottom water masses is reproduced as is their meridional spreading. Most prominent, the northward erosion of the AAIW, marked by its slowly increasing salinity minimum toward the north and the accompanying decrease of the layer thickness, is reproduced by the model. The subsurface salinity maximum is attributed to the NADW that is characterized by its southward extension into the Argentine Basin. Since no restoring to climatologies of T and S has been applied below the sea surface during the integration, the model tracer fields may deviate from their initial distribution. By the end of the reference experiment, for example, the upper ocean was colder and fresher, the intermediate water was warmer and saltier, and the deep waters were slightly warmer than at the beginning of the experiment.

4. Drifter Data

In this section the model flow field in 90 m depth is compared to a velocity field derived from surface drifter data. Before discussing this in detail, the data set itself is briefly introduced.

As part of the World Ocean Circulation Experiment (WOCE) field program, 273 surface drifters were deployed in the South Atlantic Ocean and the southwestern Indian Ocean between 1990 and 1995. *Schäfer and Krauss* [1995] analyzed in detail the then available data set with respect to the South Atlantic eddy statistics. All buoys were equipped with a drogue in 100 m depth to ensure that they follow the quasi-geostrophic dynamics below the surface Ekman layer. *Krauss et al.* [1989] showed that undrogued buoys tend to move faster as a consequence of the dominant wind forcing in the absence of a drogue. This leads to kinetic energy levels much too high to be representative of the geostrophic flow. To prevent a contamination of the data set by undrogued buoys, only those data were withheld that were recorded before a drifter lost its drogue. In most cases the separation of the time series into drogued and undrogued parts could be done directly from the raw data. Ambiguous parts of the time series were examined following the method discussed by *Brügge and Dengg* [1991] and rejected in doubtful cases. The remaining trajectories of the drogued drifters are depicted in Figure 5. While the buoys are concentrated in the regimes of the boundary currents, in the tropical and southwestern South Atlantic there exist vast areas with no data coverage at all like the region west of the Agulhas Retroflection area and the tropical South Atlantic northeast of the South Equatorial Current (SEC), respectively.

The derivation of quasi-Eulerian velocities from the drifter data requires the application of a suitable interpolation method that provides a velocity field on the regular model grid. A statistically reliable mean velocity field on the model grid could be obtained with a relatively simple averaging approach: it was created by computing means of all available data inside a horizontal box of $3° \times 3.6°$ in latitude and longitude, respectively, with its center on a model grid point. This was done for every grid point. The distance of the data points inside the averaging box to its center was taken into account by using a linear weighting function. This diminishes the fact that one data point may influence the mean values at up to nine model grid points. By this method a mean velocity was obtained as far as observed data were available. This mean field is not yet a statistically reliable result because of neglecting any Lagrangian timescale and a stability criterion for the mean values. By using a Lagrangian timescale of 2 days and rejecting all of those mean values computed with less than 100 independent

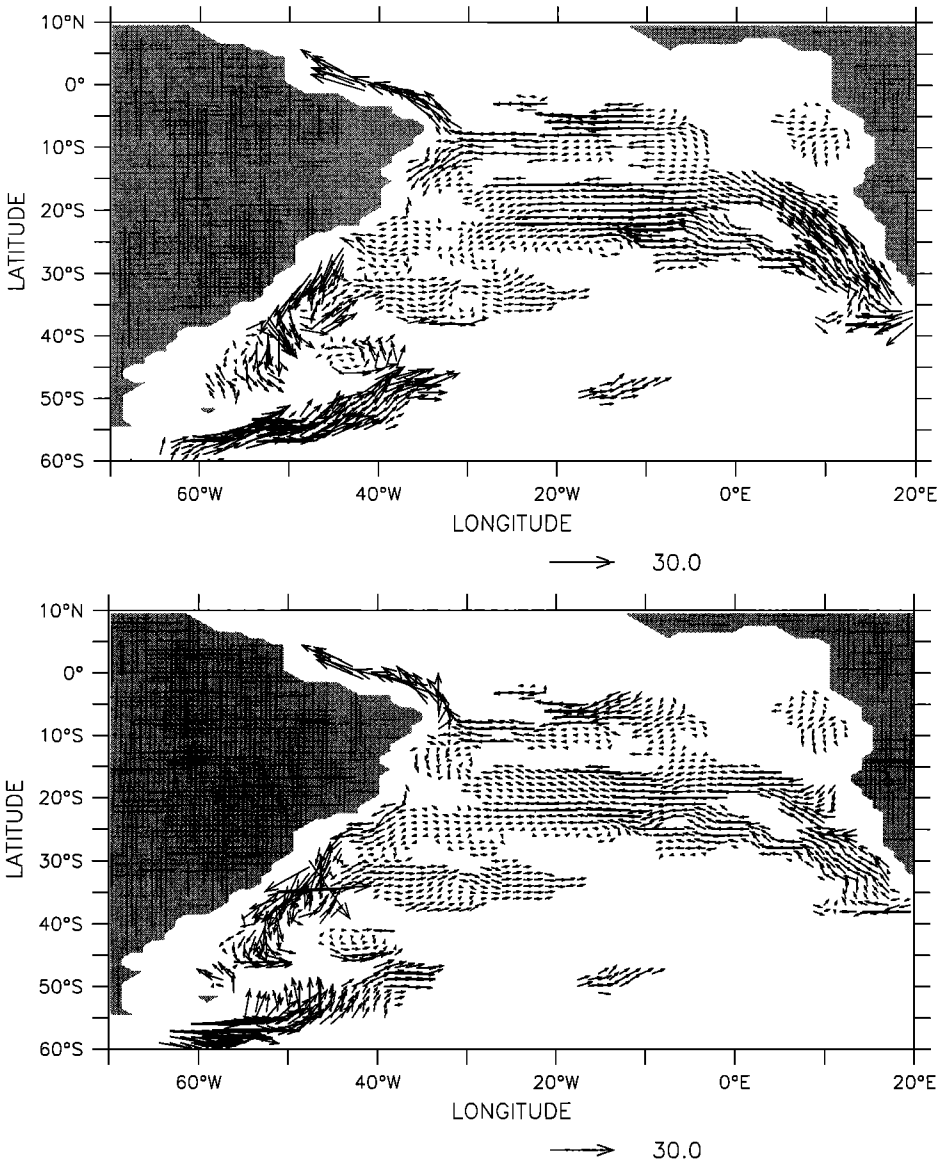

Figure 6. (top) Mean velocity field derived from the drifter data set. (bottom) Velocity field at 90 m depth from the reference model at the same locations where observed data are available.

buoy days, a statistically reliable mean velocity field is obtained. This meets approximately the conditions for statistically stable mean velocities derived from drifter data as discussed by *Brügge* [1995] for equally sized boxes in the North Atlantic and by *Schäfer and Krauss* [1995] for boxes of varying shape in the South Atlantic.

The resulting mean field is shown in Figure 6 (top). The flow field is not free of divergences. They are small, however, and have only a minor effect on the model results as discussed below. A comparison with the drifter trajectories shows where the data coverage was sufficient for deriving mean velocities. Thus one observes well-developed currents like the Benguela Current, South Equatorial Current, and Antarctic Circumpolar Current west of 30°W. The Brazil Current and the Malvinas/Falkland Current are less well developed, and the southern boundary of the subtropical gyre is missing altogether. There and in other vast areas of the South Atlantic the data coverage was not adequate to compute averages.

This mean velocity field serves from now on as an observed mean state of the South Atlantic circulation in 100 m depth. While it may seem premature to use this flow field in the model and leaving large gaps in the circulation scheme, we nevertheless made the assimilation experiment with this mean field because it is as close as possible to the original drifter data set. An additional objective analysis does close many of the gaps in the subtropical gyre but introduces additional features such as meanders in the large-scale flow field that are the result of the statistical analysis rather than grounded in physical arguments.

A comparison with the velocity field in approximately the same depth from the reference model run depicted in Figure 6 (bottom) reveals some remarkable differences. One is the weak Benguela Current in the model which appears stronger in the observed data. Another is the broad northwestward flow of the SEC that contradicts the almost zonally flowing SEC as measured by the drifter data. Finally, we stress the weak link between the ACC and Brazil-Malvinas Confluence Zone which is restricted to the westernmost part of the Falkland Plateau in the drifter data and is almost absent east of 55°W, while it is

well established in the model. This missing link between the Malvinas Current south of the confluence region and the ACC after leaving Drake Passage is a striking feature that appears also in other data sets from surface drifters. It can be observed in our buoy data set as well as, for example, in the First Global Atmospheric Research Program Global Experiment (FGGE) drifter data set [see *Hofmann*, 1985; *Johnson*, 1989]. While there is no continuous Malvinas Current observed near the sea surface, it is well established in greater depth as documented by Autonomous Lagrangian Circulation Explorer (ALACE) floats [*Davis et al.*, 1996].

5. Numerical Experiments: Assimilation Experiment

The strong coupling of the horizontal velocity at one model level to a velocity field derived from surface drifter data prevents a free evolution of the flow field at the directly affected level. It is ensured, instead, that the model remains there close to the imposed state. Therefore the assimilation is alternatively called relaxation. The model levels above and below are not directly disturbed, although an indirect influence keeps working through the vertical advection and diffusion of momentum. In the following the effect of this assimilation is discussed in comparison with the corresponding results from the reference run. This will be done by reviewing the effects of the assimilation from the regional scale of a South Atlantic subdomain to integrated quantities of the entire South Atlantic.

The discussion is first restricted to the area where optimal data coverage is achieved. This is the case for the central subtropical gyre as shown in Figure 7. The mean velocity fields of the reference run and the relaxation run are depicted in Figures 7, top and bottom, for the third model level (centered at 90 m) and for level 9 (centered at 474 m), respectively. Near the sea surface the relaxation causes a generally enhanced flow and a different orientation of the circulation in comparison to the standard experiment. This is an anticipated result, as the assimilation method forces the model to adapt closely to the observed, predominantly westward flow in this region. At 474 m depth the assimilation has a still visible remote effect on the circulation, although significantly reduced with regard to the near-surface flow. This is to be expected, too, because the direct influence of the observed data on the model momentum balance decreases with increasing depth.

The coupling to the velocity data affects the tracer distribution as shown in Figure 8. Along a zonal section the differences between the mean modeled temperature from the reference run and the annual mean temperature climatology of *Levitus* [1982] (Figure 8, top) and between the temperature from the assimilation run and the climatology (Figure 8, bottom) are displayed. The section is located at 19°S between the bounding longitudes of the region shown in Figure 7 and extends over the upper 900 m of the ocean. The comparison between the reference run and the climatology indicates a drift of the model tracer field during the integration of the spin-up and the reference experiment. Deviations of more than 2°C emerge as the model tends to cool the upper 100 m and to warm the thermocline waters between 200 and 700 m depth.

The assimilation of velocity data has an ambiguous effect on the temperature distribution. On the one hand, it appears as an enhanced cooling of the directly affected layer in 90 m depth of up to 4°C as compared to the climatology. This decrease of temperature near the sea surface is a result of the strong Benguela Current that appears in the observed data set. The assimilation intensifies this current in the model. This strengthening is only partly caused by a stronger advection of water from the AC. It is also attributed to an intensification of the nearshore flank of the current that causes cooler upwelled water to be fed into the Benguela Current, leading to a stronger northwestward advection of relatively cold water. The model does not properly resolve the narrow upwelling zone and the coastal upwelling jet. However, the integrated effect of the upwelling is included; that is, the general eastward decrease of temperature and the upward sloping of isotherms in the upper ocean near the African Shelf are observed in the model. While this cooling seems to indicate a worsening of the model results with respect to the climatological data set, there appears, on the other hand, a smaller model-data difference in levels below where the warming trend, as observed in the reference model, is reduced to 1.5°C and less.

In addition to the stronger horizontal advection, the data assimilation causes divergences of the flow field. This is problematic, especially in the transition regions between areas where observed data are available and those where this is not the case. The vertical velocities induced in the transition zones may lead to an enhanced vertical advection of tracers, thus slowly reshaping the density structure. However, the thermocline limits this effect in the vertical. Therefore it is more appropriate to look at the influence of the assimilation on the warm water sphere as a whole rather than on a single section. Let us define the warm water sphere by the thickness of the water column with a minimum temperature of 9°C (or, equivalently, the depth of the 9°C isotherm). This is depicted in Figure 9 (top to bottom) for the reference model, the assimilation run, and the climatology of *Levitus* [1982], respectively. Obviously, the relaxation of velocity data increases the thickness of the warm water pool in the central subtropical gyre and stretches it to the east. This structure is similar to that observed in the climatology. In the assimilation experiment the stronger Benguela and South Equatorial Currents are responsible for the intensified flow within the subtropical gyre, while there is only a small additional contribution to the northward flowing North Brazil Current. The enhanced anticylonic flow deepens the warm water cell. This is in contrast to the result derived from the reference run, where the warm water sphere is comparatively shallower and its maximum thickness is restricted to the region west of the Mid-Atlantic Ridge.

The intensified flow of the subtropical gyre interior can also be identified in Figure 10. Depicted is the difference of the amplitudes of the barotropic stream function from the reference and relaxation experiments. Negative values indicate a higher absolute stream function value in the relaxation run and vice versa. The image may be divided into three regions, namely, the subtropical gyre with higher values from the relaxation run, the domain of the SAC where it produces slightly lower values, and the ACC where the relaxation experiment has lower stream function amplitudes. The last feature is mainly a result of the Malvinas Current which is absent in the drifter data set. This, in turn, weakens the northern part of the ACC in the relaxation experiment. This is reflected by the decreased stream function amplitude as compared with the reference experiment.

The increased amplitude of the subtropical stream function field in the northern and central subtropical gyre as a consequence of the assimilation indicates the momentum input by the observed velocity data. However, the stream function dif-

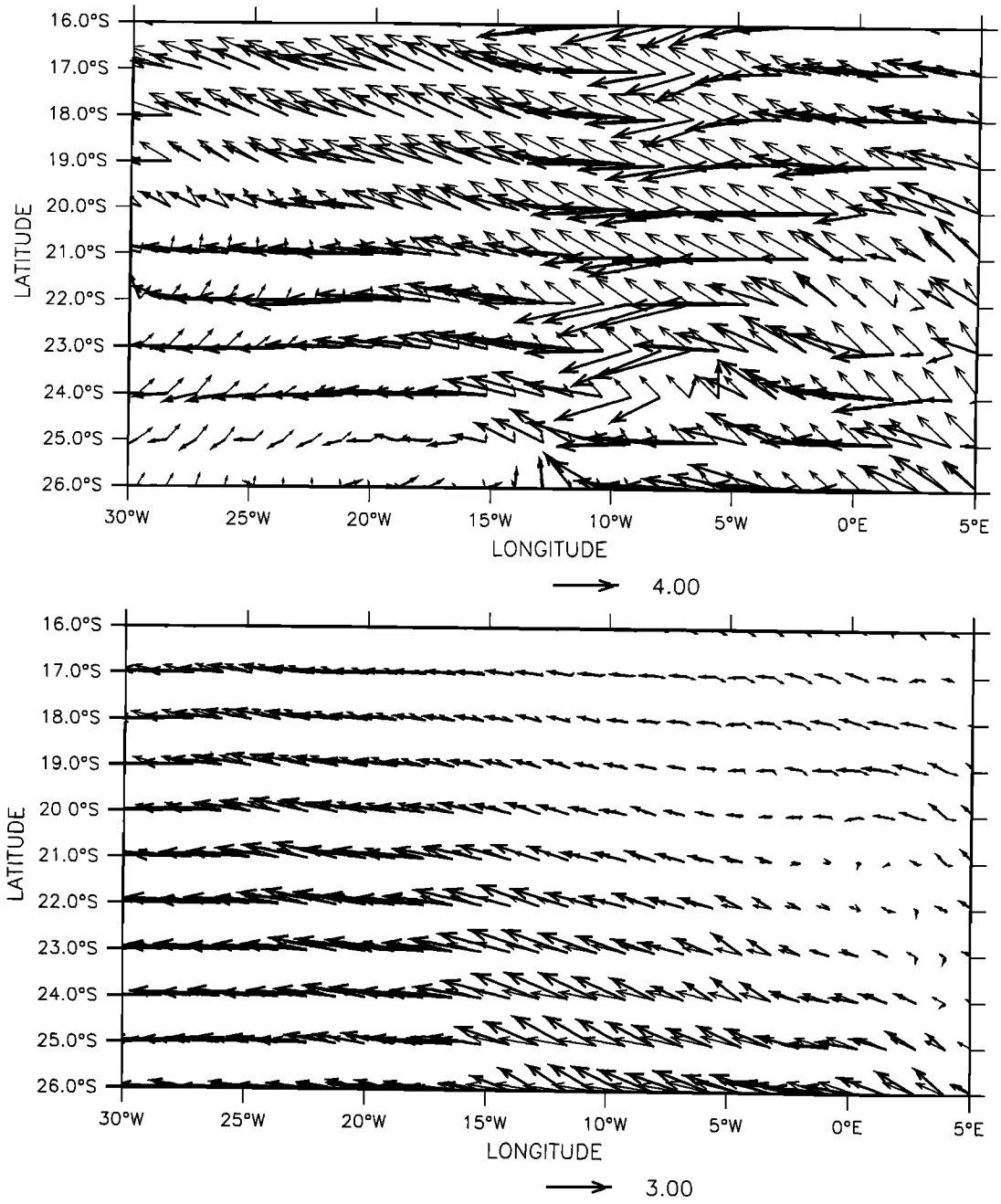

Figure 7. Velocity fields in the central subtropical gyre at (top) 90 m depth and (bottom) 474 m depth. Thin arrows denote the reference model; bold arrows denote those computed during the assimilation experiment.

ferences between the two model realizations are small in the vicinity of the subtropical front. It follows that the horizontal gradients across the gyre and thus the barotropic velocities within it are intensified by the assimilation procedure.

5.1. Meridional Volume Transport

The thermohaline-driven meridional overturning circulation is shown in Figure 11 for the standard experiment. The dominant water masses (northward flowing AAIW and NADW, directed southward) are easily identified. Approximately 15 Sv of NADW are crossing the equator southward, while about 4 Sv of AAIW are transferred to the North Atlantic. A northward transport of AABW is almost nonexistent as a consequence of limited AABW production in the Southern Ocean and the topographic blocking of a deep northward flow from the Argentine into the Brazil Basins.

Before dealing with the zonally integrated northward volume transport in more detail, we define three vertically integrated water types as suggested by *Gordon et al.* [1992]. The warm water or thermocline water is warmer than 9°C and confined to the upper 1500 m. The intermediate water encompasses the depth range between the 1500 m isobath and the 9°C isotherm or the sea surface, respectively, if there is no water warmer than 9°C. Finally, all water below 1500 m is called deep water. These definitions are somewhat arbitrary because, for example, the intermediate water includes the

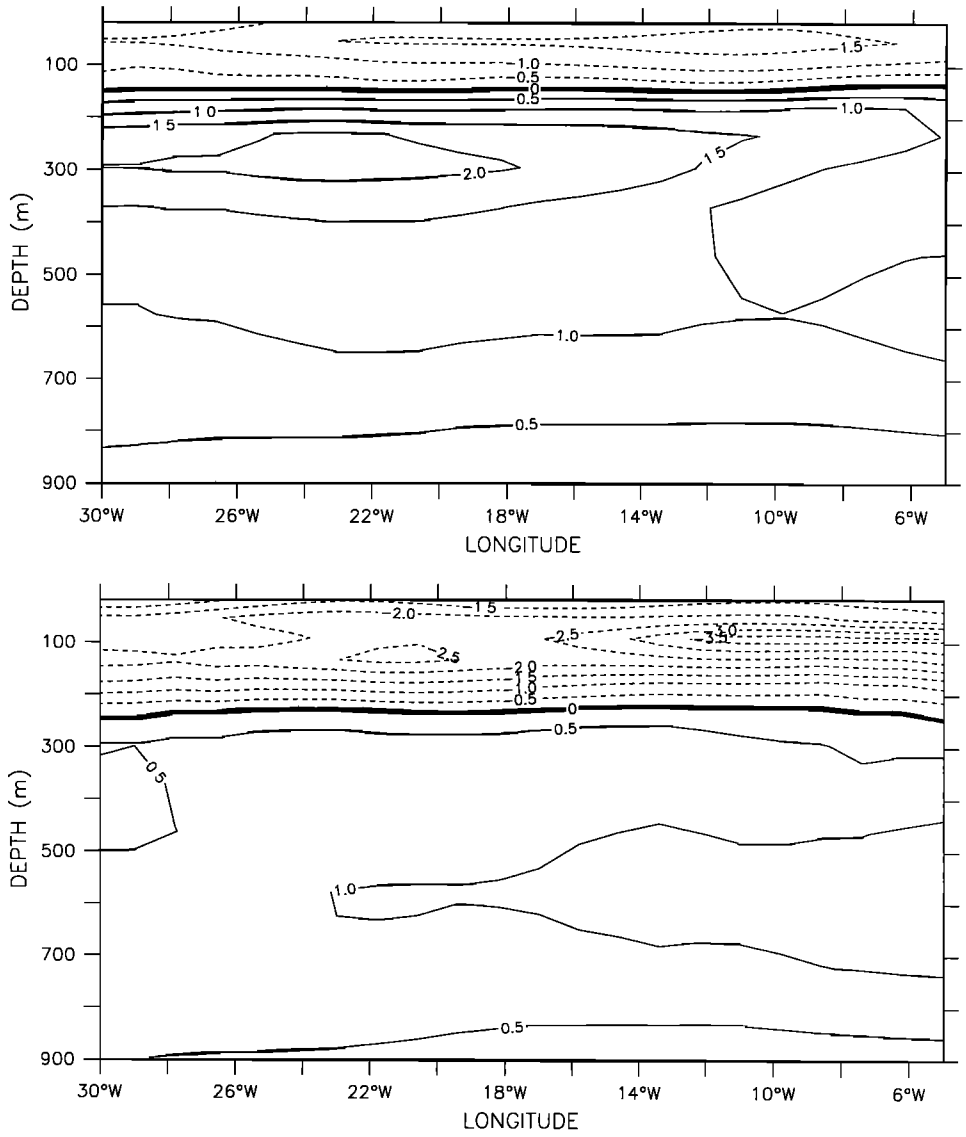

Figure 8. Differences between model-estimated temperature and the *Levitus* [1982] climatology along a zonal section at 19°S in the upper 900 m between 30°W and 5°W, showing model results from (top) the reference run and (bottom) the assimilation experiment.

whole upper ocean, south of the subtropical front, while in the north it may contain traces of NADW in the tropical Atlantic where deep water rises above the 1500 m isobath. However, to be consistent with *Gordon et al.* [1992] as well as *England and Garçon* [1994], we keep this particular water type definition.

The zonally integrated northward volume transport of surface and intermediate waters only is presented in Figure 12. In the case of the standard experiment the flow of intermediate water to the north decreases continuously from south to north, with the exception of a suddenly enhanced flow just south of 10°S, where the subtropical gyre reaches its northernmost extension near the South American coast. The transport of warm surface water behaves complementarily to the intermediate water but with a slightly weaker overall south-north gradient. This indicates the growing influence of southward flowing NADW in depths below 1000 m within the intermediate water type that accompanies the erosion of the AAIW layer to the north.

The impact of the relaxation of velocity on the northward volume transport is mainly visible south of 10°S. The stronger northward flow of warm surface water in the subtropics is almost completely balanced by the weakening of the transport of intermediate water to the north. Again, the latitude of 10°S marks the northernmost tip of the subtropical gyre where the North Brazil Current forms and effectively transports waters to the north. The more prominent effect of the assimilation south of this latitude is an indication of the already mentioned intensification of the circulation inside the subtropical gyre.

Table 2 provides volume transports across 30°/32°S, 68°W, and 20°E from different sources. The transport estimates differ considerably between the models. All simulations result in northward transports of surface and intermediate water masses. Depending on the strength of the southward flow of NADW, the relative contribution of the AAIW and surface waters to the compensating northward flow varies. Except for the reference experiment, all cited analyses result in a somewhat stronger contribution of the near-surface flow and a weaker contribution of AAIW. Generally higher transport

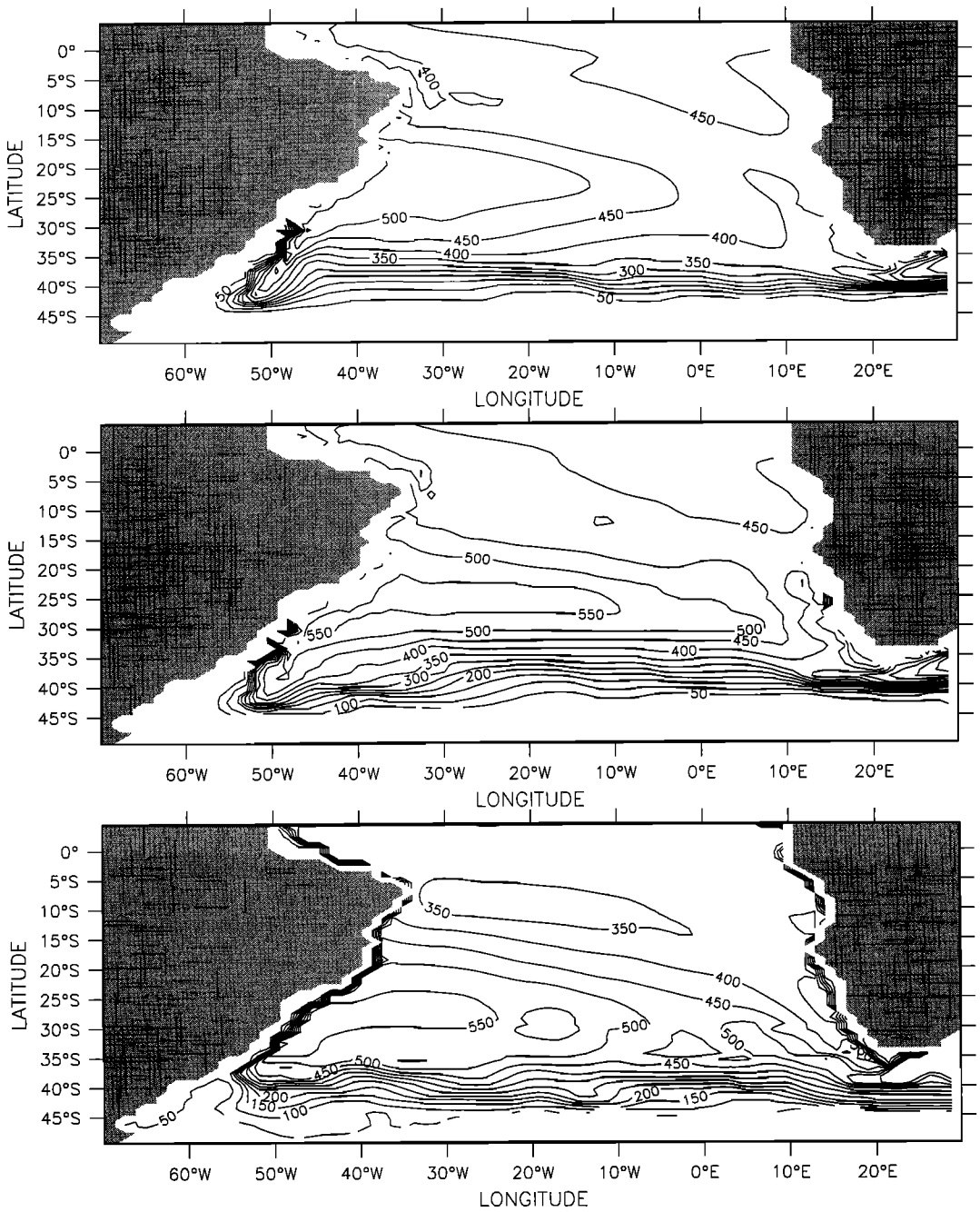

Figure 9. Depth (in meters) of the 9°C isotherm as deduced from (top) the reference model, (middle) the relaxation model, and (bottom) the *Levitus* [1982] climatology.

rates are observed for FRAM, which is the only model in this comparison that explicitly resolves mesoscale eddies.

The differences of the transport data across the meridional sections reflect the different properties of the ACC which is, in global models, often stronger than observed, while, in regional models, it depends on the boundary conditions. The data show consistently the tendency of zonally (eastward) increasing transport of deep water masses and decreasing AAIW transport, while exhibiting large differences in the actual transport rates.

The results from our model correspond well with the data from *England and Garçon* [1994] and *Marchesiello* [1995]. The former model closely matches the results from the assimilation experiment for the zonal section. The larger differences between the deep water transports across the meridional sections are attributed to the stronger ACC in the global model. For these sections we observe rather close correspondence of our results with those of *Marchesiello* [1995]. The deviating estimates for the transport within the surface layers is attributed to the definition of these layers (temperature criterion versus density criterion) and the barotropic inflow condition for the AC. The effects of differing model design, surface forcing, and lateral boundary conditions are of minor importance for the volume transports across the meridional sections.

The results from the reference and assimilation simulations deviate from the model of *Matano and Philander* [1993]. The

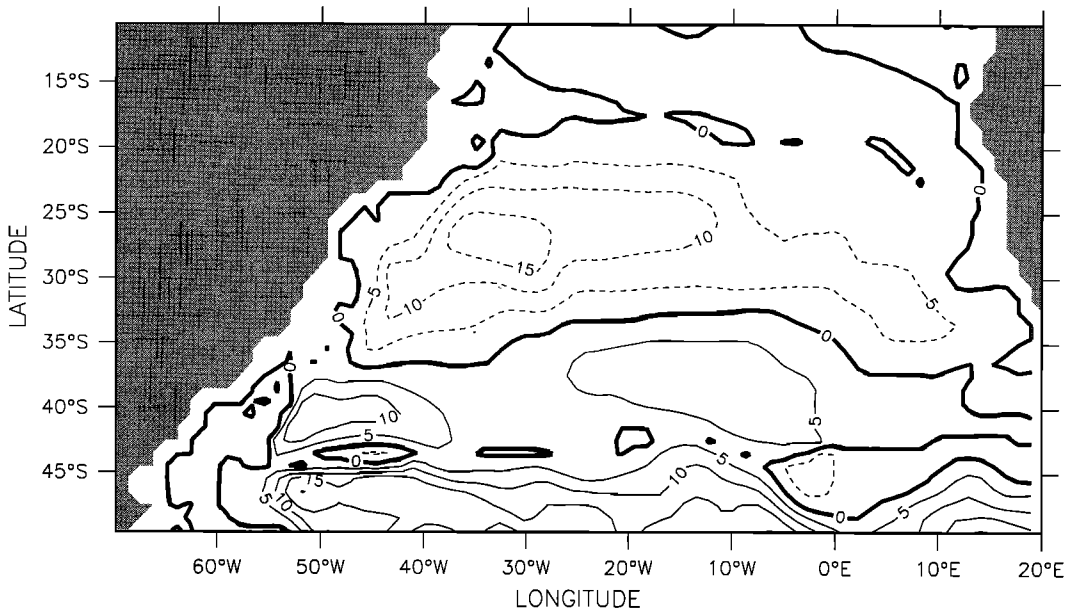

Figure 10. Difference (in sverdrups) of the stream function amplitudes from the reference and assimilation experiments.

northern boundary of their model domain is positioned at 20°S, while our model reaches well into the North Atlantic. Some of the previously shown figures indicate that the subtropical gyre in our model extends into the tropical South Atlantic north of 20°S. It represents a freely developed closed circulation that has not been forced by an adjacent boundary into its present form. In addition, the model features a Deep Western Boundary Current along the South American coast that causes the strong NADW signal and which might be weaker in the model of *Matano and Philander* [1993], where it represents mainly the situation at 20°S as it exists in the climatological boundary data set. This may lead to significantly different estimates of volume fluxes across 30°S. Differences in the open boundary conditions, in the specification of the ACC in Drake Passage, and in spatial resolution add to the deviations.

We conclude that the volume transports deduced from the reference and assimilation experiments agree generally well with other models of similar experimental design or comparable horizontal resolution. Remaining differences are due to different model types and deviating representations of bottom topography, surface forcing, and lateral boundary parameterizations, among others.

5.2. Meridional Heat Transport

The heat transport (Figure 13) derived from the model is positive (northward) throughout the subtropical and tropical South Atlantic, in accordance with most other computations.

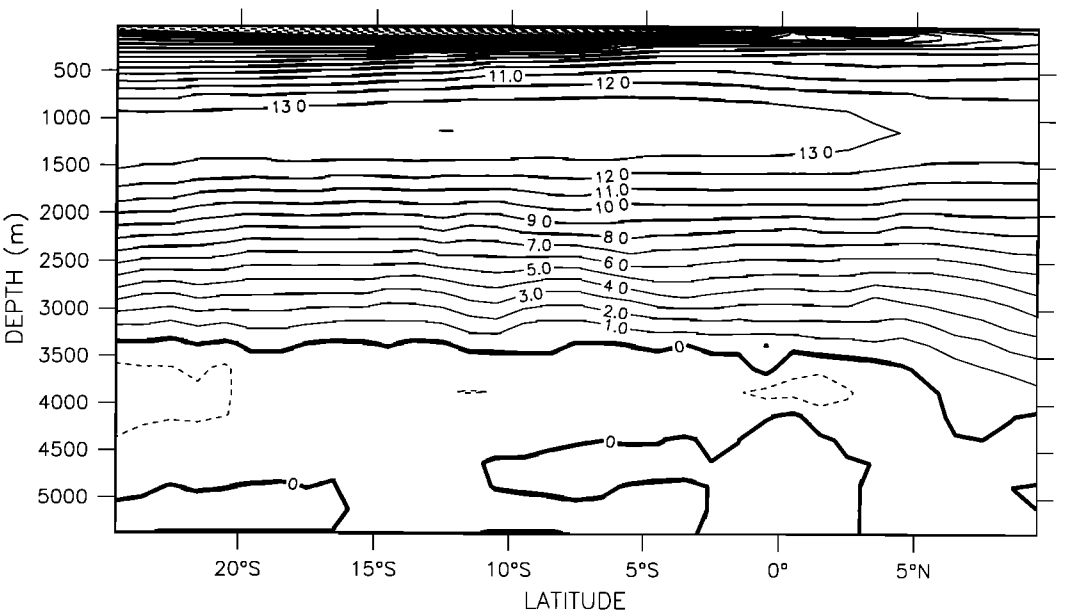

Figure 11. Meridional overturning stream function (in sverdrups) from the reference model.

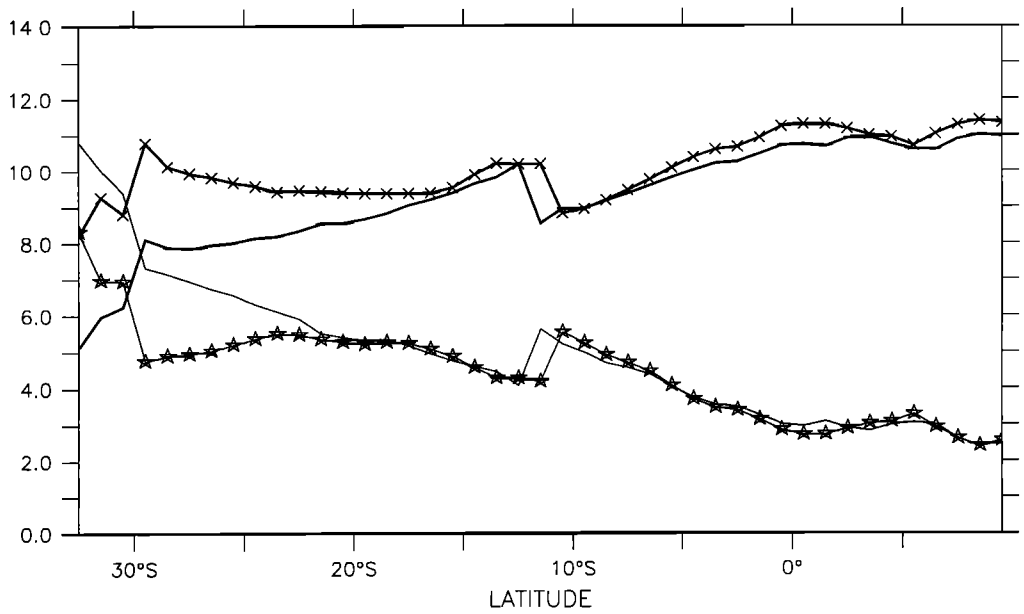

Figure 12. Zonally integrated, meridional volume transport (in sverdrups) within the warm water sphere ($T \geq 9$°C, thick lines) and the intermediate water ($T < 9$°C in the upper 1500 m, thin lines). Solid lines with symbols represent the assimilation results; solid lines are from the reference model.

South of 10°S, the heat transport is less than 0.5 PW and with only weak fluctuations. It rises in the tropics to a maximum value of 0.95 PW just north of the equator. The estimates near the equator correspond closely to those obtained by *Semtner and Chervin* [1992] northward from 10°S. The heat transports between 23° and 10°S do not match the enhanced heat transport induced by the northward component of the SEC as it exists in inverse calculations and the *Semtner and Chervin* [1992] model. Most prominent is the low value at 10°S, where the modeled heat transport is outside of the confidence range given by *Macdonald and Wunsch* [1996]. In the subtropics the model results are especially close to the inversely computed numbers and higher than in other low-resolution models. However, our model does not resolve eddies and rings that may significantly contribute to the higher meridional heat transport in the eddy-resolving models.

The change of the northward heat transport due to the assimilation of velocity data appears to be consistently higher throughout the South Atlantic. However, the difference between the two model realizations is small, indicating little influence of the relaxation on the net heat transfer from the South Atlantic to the North Atlantic.

Comparison with other estimates of the northward heat transport at distinct latitudes reveals some interesting features. Let us consider first the subtropics south of 23°S. Our model results fit well into the data range defined by previous investigators (see Figure 13 caption). In this region the model-simulated heat transports are especially close to the values obtained through inverse modeling by *Holfort* [1994] and *Macdonald and Wunsch* [1996]. However, the heat transport across approximately 30°S varies strongly among the different analyses. The eddy-resolving models generally produce a higher northward heat transport, while models of medium horizontal resolution have a tendency to yield lower heat transports. As *Thompson et al.* [1997] state, the northward heat transport in the South Atlantic depends not only on resolution but also on the inflow of Indian Ocean water via the leakage of the AC. Failing to reproduce a heat flux connected with this leakage may lead to a wrong northward heat transport. This inflow of water from the Indian into the Atlantic Ocean, in turn, depends largely on the inflow parameterization at the open boundaries in limited area models. This may explain the relatively low heat transport in the model of *Marchesiello* [1995] and the higher northward heat transports in other models that experience stronger inflow from the Indian Ocean.

6. Pathway of the NADW Compensating Flow

The South Atlantic is part of the process that is termed a "global conveyor belt" after *Broecker* [1991]. The NADW is of convective origin in the subpolar North Atlantic and leaves the Atlantic, joining the Circumpolar Deep Water within the ACC in the subpolar South Atlantic. The compensating northward flow of thermocline and intermediate waters in the South Atlantic is documented by the northward heat transport. It is caused by the northward component of the circulation in the upper 1500 m of the subtropical and tropical South Atlantic. Two different schemes have been suggested to explain this compensation, both of them received support from various numerical and inverse modeling efforts. Within the Warm Water Path (WWP), introduced by *Gordon* [1986], NADW is carried with the ACC into the Indian and Pacific Oceans, where it is upwelled into the surface waters. These thermocline waters are flowing westward via the Indonesian Archipelago (from the Pacific) and the Agulhas Current system into the South Atlantic and are eventually transported into the North Atlantic. In this scheme the influence of heat transported by the intermediate water within the ACC from the Pacific through Drake Passage into the South Atlantic is of minor importance.

On the other hand, *Rintoul* [1991] proposed that it is this transport of intermediate water by the ACC (termed Cold Water Path (CWP)) that contributes significantly to the northward heat transport. It does so by gaining heat from the atmo-

Table 2. Volume Transports Within the Warm Water Sphere (WW), the Near-Surface Ocean (SW) if a Density Criterion Was Used to Define Water Types, the Intermediate Water (IW), and the Deep Water (DW) as Defined in Text

Water Mass	Volume Transports V		
	Across 30°/32°S	Across 20°E	Across 68°W
	England and Garçon [1994]		
WW	9	−2.5	0
IW	8	95.5	110
DW	−17	70	53
	Reference Experiment		
WW	6	−2	0
IW	9	98	102
DW	−16	34	28
	Assimilation Experiment		
WW	9	−2	0
IW	7	95	104
DW	−16	37	26
	Marchesiello [1995]		
SW*	6	3	1
IW*	5	96	107
DW*	−11	30	22
	Matano and Philander [1993]		
SW*	7	3	2
IW*	2	59	67
DW*	−8	58	51
	Rintoul [1991]		
SW*	8	3	3
IW*	5	71	83
DW*	−13	55	43
	Saunders and Thompson [1993]		
SW*	13		
IW*	6		
DW*	−19		

Transports (in sverdrups) have positive values if the flow is to the east across the meridional sections (68°W and 20°E) and to the north across the zonal section (30°S/32°S).

*These water mass definitions differ from others in the table; see respective sources cited.

sphere in the outcrop regions of AAIW within the South Atlantic. This effect surpasses the heat import of Indian Ocean thermocline water from the Agulhas Current system.

As shown in this section, our model slightly favors the WWP. That is, both pathways coexist with different effects in the model, the WWP dominating the heat flux and the CWP strongly influencing the salt balance.

Consider first the heat transport across the zonal section along 30°S in Figure 14 (bottom). The solid line denotes the vertically integrated heat transport as a function of longitude. The symbols are representative of heat transports that are vertically integrated over a certain depth range only, as described in the Figure 14 caption. The section is characterized by the peak caused by the northward Brazil Current recirculation between 35° and 30°W and the broad northward heat flux eastward across the entire subtropical gyre with a maximum near 10°E. The Brazil Current itself has been omitted from Figure 14 because the discussion is restricted solely to the northward heat transport. Three different regimes may be identified. The first one is the aforementioned Brazil Current recirculation where the intermediate water contributes most of the northward heat transport. Second, in the subtropical gyre interior the heat flux is more or less equally split among the three depth ranges. It is worth noting that the heat flux east of the Mid-Atlantic Ridge is significantly higher than west of it. The third region is in the vicinity of the eastern boundary current that transports heat concentrated in the upper layers northward.

The northward heat flux across 30°S is supplied from the south mainly by the inflow from the Agulhas Current system. The argument is as follows: the import of heat by the ACC through Drake Passage is concentrated in intermediate depths as shown in Figure 14 (top). In this depth range the ACC carries roughly 50% of its total eastward heat transport. Most of it leaves the South Atlantic again while crossing the section at 20°E eastward (Figure 14, middle). There the difference between the full depth integrated heat transport and the one integrated over the upper 1500 m is attributed to the outflowing NADW. The AC contributes heat into the South Atlantic in surface, thermocline, and intermediate depths in almost equal parts. Altogether, the contributions of the surface and thermocline waters from the Indian Ocean into the South Atlantic dominate the influence of AAIW in a ratio of order 2:1. The assimilation of velocities derived from drifter data enhances further the dominance of the WWP by intensifying the near-surface inflow of Indian Ocean water at 20°E (not shown).

While the analysis of the heat fluxes seems to indicate the dominance of the WWP, this impression has to be modified when taking salt transports into account too. Presented in Figure 15 are sections of salt fluxes across 20°E and 33°S. A similar representation of the heat fluxes (not shown) exhibits the concentration of the eastward heat flux in the upper 600 m of the AC and a northward, surface-intensified heat flux in the subtropical South Atlantic east of the Mid-Atlantic Ridge (MAR). The eastward salt transport of the AC encompasses a much larger depth range. Though decreasing in strength with depth, the area of westward flow broadens to a maximum around 1000 m depth, well in the core AAIW. This flow is diverted into the subtropical South Atlantic in a strong eastern boundary current which is concentrated near the sea surface and restricted almost completely to the African Shelf. A moderate but deep reaching transport of salt is observed east of 10°W. Again, it is attached to the core of the AAIW at 1000 m depth. West of the MAR, there is (except for two limited areas with northward flow maximums) only weak salt transport to the north, if at all.

Combining and quantifying the heat and salinity analysis reveals that across 33°S, 65% of the northward heat transport is attributed to the upper ocean above 550 m depth, with a 35% share of AAIW between 550 and 2000 m depth. However, the salt transport in the intermediate depth range outweighs slightly the importance of the salt transport in the thermocline and surface waters in a ratio of 55% to 45%. Together, the results show that both pathways are relevant to the compensation of the NADW outflow, though their respective effects on heat and salt balances are fairly different.

While the inflow in the upper ocean is often confirmed in observations [*Gordon*, 1986, *Garzoli and Gordon*, 1996] and other models [*Stevens and Thompson*, 1994], there remains the need for further discussion on the role of the intermediate water. Our model indicates that AAIW has a considerable share in the import of heat into the South Atlantic within the AC leakage. Though this water is of Pacific origin, it does not

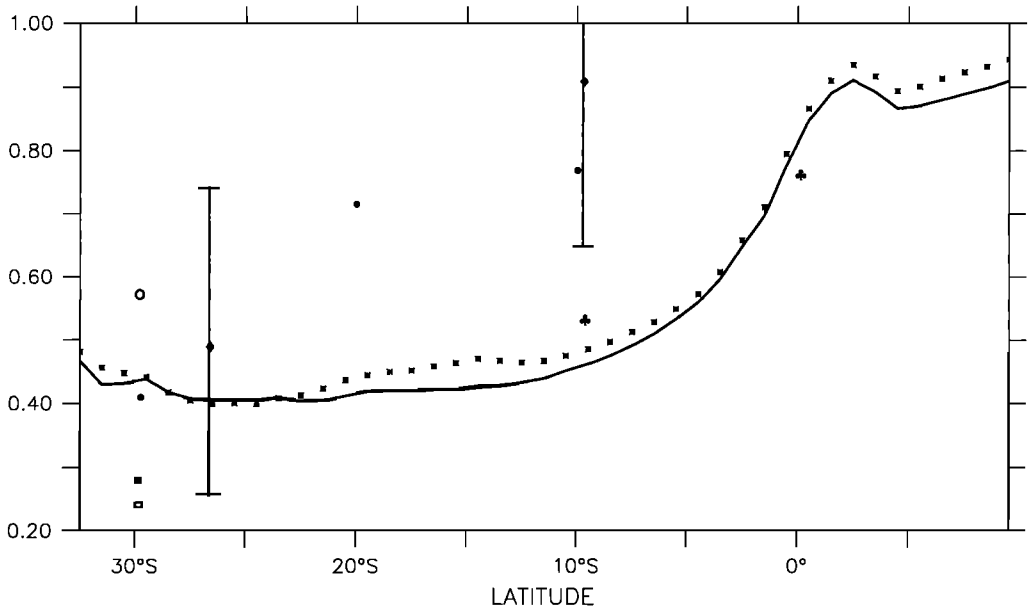

Figure 13. Meridional heat transport in 10^{15}W from the reference experiment (line) and the assimilation experiment (asterisks) between 33°S and 10°N. Symbols represent estimates from other studies as follows: open circle, *Stevens and Thompson* [1994]; open square, *Rintoul* [1991]; solid square, *Marchesiello* [1995]; cloverleafs, *Semtner and Chervin* [1992]; solid circles, *Holfort*, [1994]; and diamonds, confidence limits from *Macdonald and Wunsch* [1996]. The error bar also applies to the data of *Holfort* [1994] which have been omitted for clarity.

penetrate the subtropical South Atlantic west of the Mid-Atlantic Ridge as suggested by *Rintoul* [1991]. Rather, it follows closely the path of the ACC and partly recirculates in the Indian Ocean to flow westward within the AC. The only region in the western South Atlantic where a considerable heat transfer from subpolar to subtropical regions may occur is the Brazil-Malvinas Confluence Zone, but the model results do not give a hint that a heat exchange really happens there.

The prevailing inflow around South Africa is biased only slightly by the eastern boundary conditions. Once the inflow and outflow conditions for the barotropic mode and the tracers have been chosen and prescribed, disturbances resulting from boundary effects are confined to the viscous boundary zone. For example, an accumulation of water near the eastern boundary as a result of an incomplete dissolution of outward directed flow anomalies may occur and lead to the situation that intermediate water is sucked into the Agulhas Current system. However, this effect is small and is further eased by the relaxation toward climatological tracer data near the boundary. While this does not affect the circulation at 20°E, the initial choice of boundary data may have a considerable impact on the transfer of Indian Ocean waters into the Atlantic. For example, as has been shown by *Ou and De Ruijter* [1986], the strength of the AC is one factor that determines the location where this current retroflects. This, in turn, influences the flow of Indian Ocean water into the South Atlantic. The stronger the AC is, the farther east the retroflection of the current occurs. On the other hand, the retroflection ceases and Indian Ocean water flows along the continental shelf into the Atlantic if the AC is weak.

7. Conclusions

In this paper it has been demonstrated that a climatologically forced, limited domain, noneddy-permitting numerical model is capable of reproducing the essential characteristics of the South Atlantic mean circulation and hydrography.

The assimilation of velocity data derived from a surface drifter data set led to an improved representation of large-scale features, as the structure of the subtropical warm water sphere. The meridional heat transport is consistently higher in the assimilation experiment than in the reference run, although the quantitative differences between the two model realizations are small. In accordance with most other model results, we deduced a positive (northward) meridional heat transport throughout the South Atlantic, north of 33°S. Referenced with inversely calculated estimates, the modeled heat transport is reproduced especially well in the subtropical ocean and near the equator while discrepancies arose in the tropics off the equatorial belt.

On regional and local scales, however, the assimilation of velocity data proved to be problematic: the incomplete data coverage in combination with the chosen assimilation method generated strong divergences of the flow field, especially at the rim of the observed velocity field. This led to locally unrealistic tracer distributions. We believe that the patchy distribution of the observed velocities is the main reason for the local deformation of the density structure which, in turn, is due to the divergences between observations and model. Future experiments will concentrate on the assimilation of velocity data that are objectively analyzed before the assimilation. While this data preprocessing may generate additional flow patterns, it will reduce or even eliminate divergent flow.

The analysis of the modeled hydrography and flow field documented the role of the South Atlantic as part of the global thermohaline circulation. The flow of heat and salt within the NADW into the Indian Ocean has to be balanced by return flow in intermediate and surface layers. The AAIW flows into the South Atlantic within the ACC through Drake Passage as

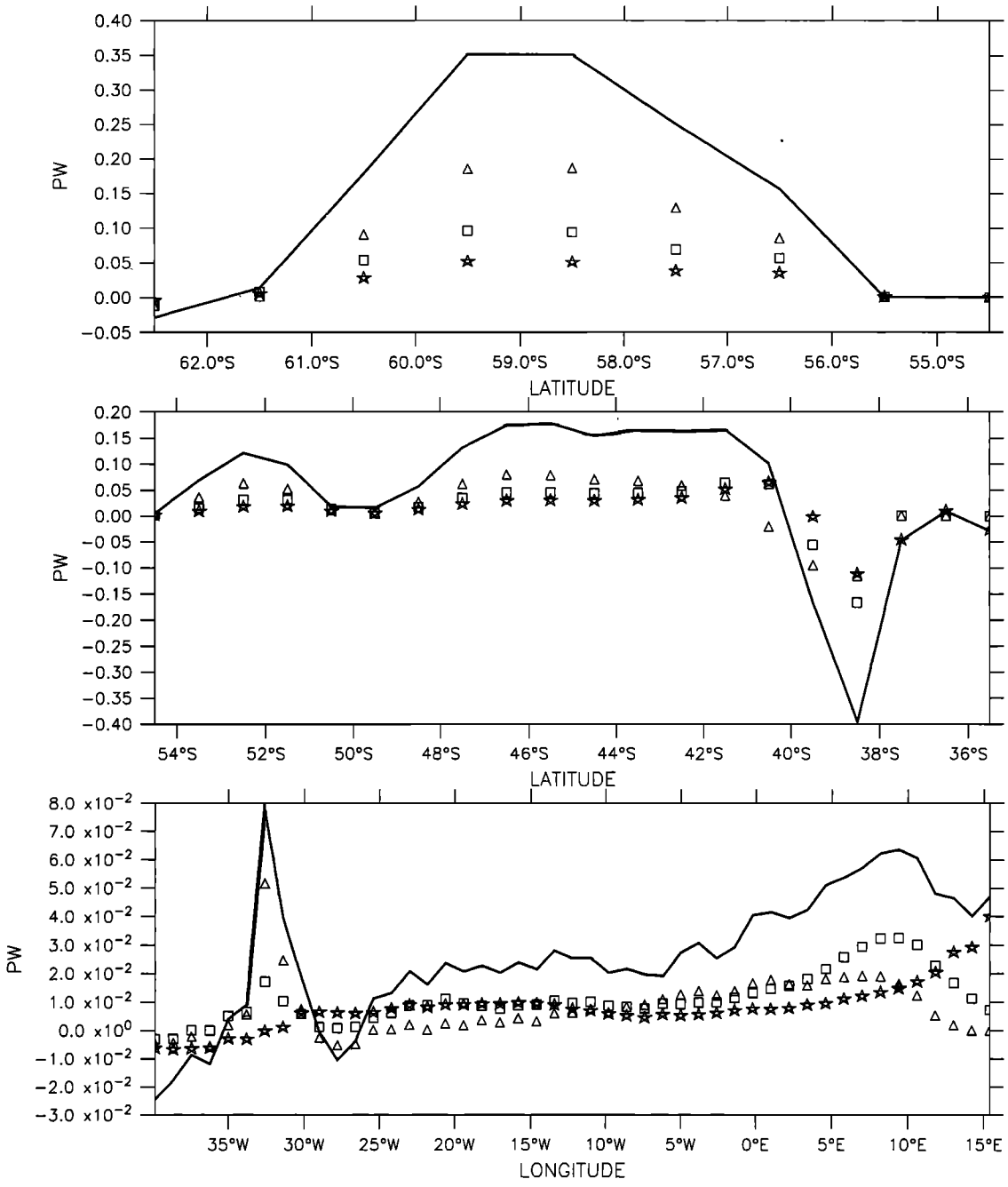

Figure 14. Heat transport in peta watts across sections along (top) 68°W, (middle) 20°E, and (bottom) 30°S from the reference experiment. The solid lines represent the full depth-integrated transport across the respective section. The heat transports integrated over the top 100 m and over the depth ranges of 100 to 500 m and 500 to 1500 m are indicated by stars, squares, and triangles, respectively.

well as in a recirculation within the AC south of South Africa. It has been shown that the latter path dominates the inflow of AAIW. It leaks into the South Atlantic below the warm Indian Ocean surface water. The AAIW is of crucial importance for the salt balance, while the surface and thermocline waters dominate the heat flux from the Indian into the Atlantic Ocean. The mixing of AAIW across the ACC and the subtropical front into the subtropical ocean is less pronounced. Both analyses combined suggest a slight dominance of the so-called "warm water path."

Certainly, one has to keep in mind the coarse resolution of the model grid and the simplified lateral boundary conditions, so that this estimate should be interpreted merely as a preliminary suggestion that might be revised in future models. An increased and eddy-resolving horizontal resolution may considerably improve the model results in the Brazil-Malvinas Confluence Zone as well as in the Agulhas Retroflection area and thus allow for an eddy-induced transfer of intermediate and Indian Ocean thermocline waters into the subtropical South Atlantic.

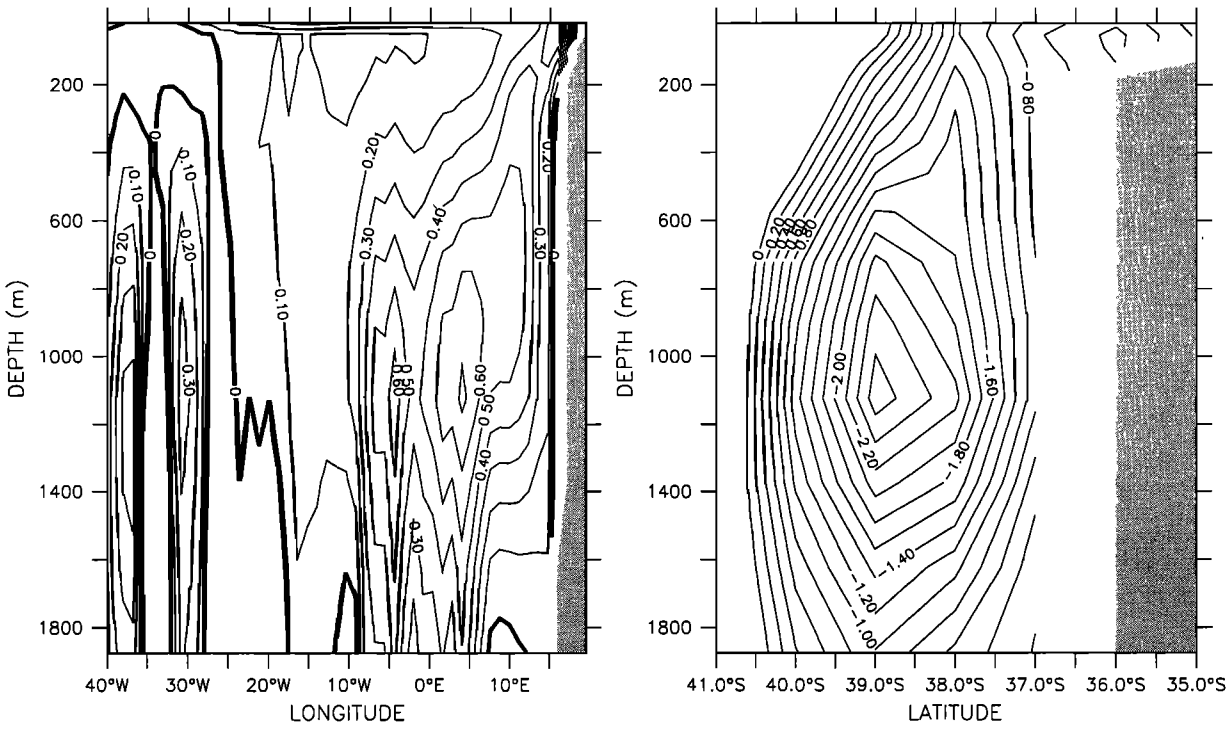

Figure 15. Sections of salt transport (in 10^{10} g/s) across (left) the subtropical South Atlantic east of the Brazil Current and its recirculation at 33°S and (right) the Agulhas Current at 20°E.

Acknowledgments. This paper is a contribution to the German WOCE, supported by the Bundeministerium für Forschung und Technologie under contract 03F0121A. Figures have partly been drawn with *Ferret*. The work of two anonymous reviewers is gratefully acknowledged. The manuscript received major improvements and additional features based on the suggestions of one of them.

References

Broecker, W. S., The great ocean conveyor, *Oceanography*, *4*, 79–89, 1991.

Brügge, B., Near-surface mean circulation and kinetic energy in the central North Atlantic from drifter data, *J. Geophys. Res.*, *100*, 20,543–20,554, 1995.

Brügge, B., and J. Dengg, Differences in drift behavior between drogued and undrogued satellite-tracked drifting buoys, *J. Geophys. Res.*, *96*, 7249–7263, 1991.

Bryan, K., A numerical method for the study of the circulation of the world ocean, *J. Comput. Phys.*, *4*, 347–376, 1969.

Clement, A. C., and A. L. Gordon, The absolute velocity field of Agulhas eddies and the Benguela Current, *J. Geophys. Res.*, *100*, 22,591–22,601, 1995.

Cox, M. D., A primitive equation, 3-dimensional model of the ocean, *Tech. Rep. 1*, Geophys. Fluid Dyn. Lab., Princeton Univ., Princeton, N. J., 1984.

Davis, R. E., P. D. Killworth, and J. R. Blundell, Comparison of Autonomous Lagrangian Circulation Explorer and fine resolution Antarctic model results in the South Atlantic, *J. Geophys. Res.*, *101*, 855–884, 1996.

Döscher, R., and R. Redler, The relative importance of northern overflow and subpolar deep convection for the North Atlantic thermohaline circulation, *J. Phys. Oceanogr.*, *27*, 1894–1902, 1997.

England, M. H., and V. Garçon. South Atlantic circulation in a world ocean model, *Ann. Geophys.*, *12*, 812–825, 1994.

Garzoli, S. L., and A. L. Gordon, Origins and variability of the Benguela Current, *J. Geophys. Res.*, *101*, 897–906, 1996.

Gordon, A. L., Interocean exchange of thermocline water, *J. Geophys. Res.*, *91*, 5037–5046, 1986.

Gordon, A. L., R. F. Weiss, W. M. Smethie Jr., and M. J. Warner, Thermocline and intermediate water communication between the South Atlantic and Indian Oceans, *J. Geophys. Res.*, *97*, 7223–7240, 1992.

Haidvogel, D. B., J. L. Wilkin, and R. Young, A semi-spectral primitive equation ocean circulation model using vertical sigma and orthogonal curvilinear horizontal coordinates, *J. Comput. Phys.*, *94*, 151–185, 1991.

Hellerman, S., and M. Rosenstein, Normal monthly wind stress over the World Ocean with error estimates, *J. Phys. Oceanogr.*, *13*, 1093–1104, 1983.

Hofmann, E. E., The large-scale horizontal structure of the Antarctic Circumpolar Current from FGGE drifters, *J. Geophys. Res.*, *90*, 7087–7097, 1985.

Holfort, J., Großräumige Zirkulation and meridionale Transporte im Südatlantik, *Rep. 260*, 96 pp., Inst. für Meereskunde, Univ. Kiel, Kiel, Germany, 1994.

Holland, W. R., and P. Malanotte-Rizzoli. Assimilation of altimeter data into an ocean circulation model, space versus time resolution studies, *J. Phys. Oceanogr.*, *19*, 1507–1534, 1989.

Johnson, M. A., Southern Ocean surface characteristics from FGGE buoys, *J. Phys. Oceanogr.*, *19*, 696–705, 1989.

Krauss, W., J. Dengg, and H.-H. Hinrichsen, The response of drifting buoys to currents and wind, *J. Geophys. Res.*, *94*, 3201–3210, 1989.

Levitus, S., Climatological atlas of the world ocean, *NOAA Prof. Pap. 13*, 173 pp., U. S. Govt. Print. Off., Washington, D. C., 1982.

Macdonald, A. M., and C. Wunsch, An estimate of global ocean circulation and heat fluxes, *Nature*, *382*, 436–439, 1996.

Marchesiello, P., Simulation de la circulation océanique dans l'Atlantique Sud, avec un modèle numérique à coordonné σ, Ph.D. thesis, Univ. Grenoble II, Grenoble, France, 1995.

Marchesiello, P., B. Barnier, and A. P. de Miranda, A sigma-coordinate primitive equation model for studying the circulation in the South Atlantic, II, Meridional transports and seasonal variability, *Deep Sea Res., Part I*, *45*, 573–608, 1998.

Matano, R. P., On the separation of the Brazil Current from the coast, *J. Phys. Oceanogr.*, *23*, 79–90, 1993.

Matano, R. P., and S. H. G. Philander, Heat and mass balances of the South Atlantic Ocean calculated from a numerical model, *J. Geophys. Res.*, *98*, 977–984, 1993.

Olbers, J. J., V. Gouretski, G. Seiss, and J. Schröter, Hydrographic

atlas of the southern ocean, Alfred Wegener Inst., Bremerhaven, Germany, 1992.

Oort, A., Global atmospheric circulation statistics, *NOAA Prof. Pap. 14*, 180 pp., U. S. Govt. Print. Off., Washington, D. C., 1983.

Ou, H. W., and W. P. M. De Ruijter, Separation of an inertial boundary current from a curved coastline, *J. Phys. Oceanogr., 16*, 280–289, 1986.

Pacanowski, R. C., K. Dixon, and D. Rosati, MOM 1 user's guide, technical report, Geophys. Fluid Dyn. Lab., Princeton, N. J., 1991.

Pacanowski, R. C., K. Dixon, and D. Rosati, MOM 2 user's guide, technical report, Geophys. Fluid Dyn. Lab., Princeton, N. J., 1995.

Redi, M. H., Oceanic isopycnal mixing by coordinate rotation, *J. Phys. Oceanogr., 12*, 1154–1158, 1982.

Rintoul, S. R., South Atlantic interbasin exchange, *J. Geophys. Res., 96*, 2675–2692, 1991.

Saunders, P. M., and S. R. Thompson, Transport, heat and freshwater fluxes within a diagnostic numerical model (FRAM), *J. Phys. Oceanogr., 23*, 452–464, 1993.

Schäfer, H., and W. Krauss, Eddy statistics in the South Atlantic as derived from drifters drogued at 100 m, *J. Mar. Res., 53*, 403–431, 1995.

Semtner, A. J., and R. M. Chervin, Ocean general circulation from a global eddy-resolving model, *J. Geophys. Res., 97*, 5493–5550, 1992.

Stevens, D. P., On open boundary conditions for three dimensional primitive equation ocean circulation models, *Geophys. Astrophys. Fluid Dyn., 51*, 103–133, 1990.

Stevens, D. P., The open boundary condition in the United Kingdom Fine-Resolution Antarctic Model, *J. Phys. Oceanogr., 21*, 1494–1499, 1991.

Stevens, D. P., and S. R. Thompson, The South Atlantic in the Fine-Resolution Antarctic Model, *Ann. Geophys., 12*, 826–839, 1994.

Stutzer, S., Modellierung der mittleren Zirkulation im Sudatlantik. *Rep. 287*, 130 pp., Inst. für Meereskunde, Univ. Kiel, Kiel, Germany, 1997.

The FRAM Group, An eddy-resolving model of the Southern Ocean, *Eos Trans. AGU, 72*, 174–175, 1991.

Thompson, S. R., D. P. Stevens, and K. Döös, The importance of interocean exchange south of Africa in a numerical model, *J. Geophys. Res., 102*, 3303–3315, 1997.

Tsuchiya, M., L. D. Talley, and M. S. McCartney, Water-mass distributions in the western South Atlantic; A section from South Georgia Island (54S) northward across the equator, *J. Mar. Res., 52*, 55–81, 1994.

Whitworth III, T., and R. G. Peterson, Volume transport of the Antarctic Circumpolar Current from bottom pressure measurements, *J. Phys. Oceanogr., 15*, 810–816, 1985.

Whitworth III, T., W. D. Nowlin Jr., and S. J. Worley, The net transport of the Antarctic Circumpolar Current through Drake Passage, *J. Phys. Oceanogr., 12*, 960–971, 1982.

Woodgate, R., The effects of assimilation on the physics of an ocean model, II, Baroclinic identical-twin experiments, *J. Atmos. Oceanic Technol., 14*, 910–924, 1997.

W. Krauss and S. Stutzer (corresponding author), Institut für Meereskunde Kiel, Düsternbrooker Weg 20, 24105 Kiel, Germany. (sstutzer@ifm.uni-kiel.de)

(Received September 9, 1997; revised May 5, 1998;
accepted June 16, 1998.)